ANALYSIS OF ERROR PROPAGATION IN QUANTUM COMPUTERS

ZIANG YU AND YINGZHOU LI

ABSTRACT. Most quantum gate errors can be characterized by two error models, namely the probabilistic error model and the Kraus error model. We proved that for a quantum circuit with either of those two models or a mix of both, the propagation error in terms of Frobenius norm is upper bounded by $2(1 - (1 - r)^m)$, where $0 \leq r < 1$ is a constant independent of the qubit number and circuit depth, and m is the number of gates in the circuit. Numerical experiments of synthetic quantum circuits and quantum Fourier transform circuits are performed on the simulator of the IBM Vigo quantum computer to verify our analytical results, which show that our upper bound is tight.

1. INTRODUCTION

Quantum computing has been developing rapidly in recent years. It has been shown that for some specific tasks, quantum algorithms are faster than their classical counterparts, including Deutsch-Jozsa algorithm [6], Simon algorithm [16], Schor algorithm [14], Grover algorithm [10], etc. However, limited by the current quantum hardware technology, quantum computers suffer from loads of noise and errors, e.g., depolarization, decoherence, readout error, etc. For quantum circuits with large depths, the results are not reliable. The current status of quantum computing is known as the noisy intermediate-scale quantum (NISQ) era [8], which could last for many more years.

There are various errors in executing a quantum algorithm on a quantum computer. We group them into three categories: quantum algorithm approximation error, quantum sampling error, and quantum machine error. Quantum algorithm approximation error is due to the approximation in representing the original models or problems in the algorithm design. One typical example is the Trotter error in the quantum phase estimation algorithm. Quantum sampling error is due to the population mean in approximating the underlying wavefunction coefficients. Quantum machine error is due to imperfect hardware, where the major source is caused by the interaction of the quantum computer with its surrounding environment. Throughout this paper, we refer to the quantum machine error as the quantum error and discuss its propagation behavior.

Numerous methods have been proposed to mitigate quantum error. We group these methods into two categories: quantum error correction and quantum algorithm design. Quantum error correction adopts quantum syndrome measurement to provide information about whether and in what ways a qubit has been corrupted without destroying the quantum state of this logical qubit. Different quantum error correction codes have been brought forward, including Shor code [15], Calderbank-Shor-Steane (CSS) code [3, 17], additive codes [2, 4, 9], etc. From a

quantum algorithm design perspective, the noisy terms could be summed together, and by the central limit theorem, the summed error would be mitigated. For example, variational quantum eigensolver is found to be relatively robust to quantum noises [13, 18]. A similar phenomenon is observed in its closely related excited state eigensolver [1]. For all aforementioned methods mitigating quantum errors, none of them eliminates the errors. The propagation error of a noisy quantum circuit guides experiments on how large a quantum circuit is permitted given a fixed error level. For quantum error correction, the propagation error could indicate which type of error has a stronger impact on the final results. Hence, it is essential to study the cumulation and propagation of the quantum error and give a theoretical upper bound.

The propagation of quantum error has been studied under various scenarios. In [11], the convergence of continuous-time depolarizing channels was investigated in terms of relative entropy. Deshpande et al. [5] gave tight bounds on the convergence of noisy random circuits. From one perspective, noisy random circuits can be viewed as the propagation of a sequence of noisy identity gates. Flannigan et al. [7] numerically explored the propagation of quantum errors in simulating the Hubbard model and transverse field Ising model. Very differently, in this work, we study the propagation of quantum error with the Kraus and probabilistic error model.

Any quantum algorithm is first compiled into a sequence of quantum circuits and then executed on a quantum computer or quantum simulator. The execution of a quantum circuit is equivalent to applying a sequence of quantum gates on an initial density matrix. Quantum gates are unitary matrices, and applying a gate on a density matrix admits $U\rho U^\dagger$, where ρ denotes the density matrix and U is the unitary matrix associated with the quantum gate. The application of a noisy quantum gate admits $U\rho U^\dagger + \mathcal{E}$, where $\mathcal{E}$ denotes the error. For various types of quantum errors, $\mathcal{E}$ admits different properties. When a trace-preserving error is considered, $\mathcal{E}$ has trace zero, i.e., $\mathrm{tr}\,(\mathcal{E}) = 0$. Alternatively, we could also represent quantum error as $\mathcal{E}\left(U\rho U^\dagger\right)$, where $\mathcal{E}(\cdot)$ is abused as a linear error operator. For more details on the quantum error model, please refer to Section 2.

In traditional numerical analysis, e.g., numerical ordinary differential equation error analysis, the global error in terms of matrix norm grows exponentially with the number of matrices, where the matrix spectrum is assumed to be greater than one. In quantum computing, all matrices are unitary with spectrums precisely being one, and we could easily give an error bound growing linearly instead. While linear growing bound is not consistent with numerical experiments.

Figure 1 illustrates the quantum error of a Quantum Fourier Transform circuit on a quantum simulator. Instead of growing linearly, the error saturated and hit a plateau towards the end. Based on this observation, we aim to give a bound on quantum error propagation, revealing such a growing behavior.

In this paper, we analyzed the two error models: the probabilistic error model and Kraus error model, and proved their bounds of error propagation in terms of matrix Frobenius norm. Both bounds characterize the error growth behavior as in Figure 1. Then, we combined two results together and proved the following main theorem for the mixed error model.
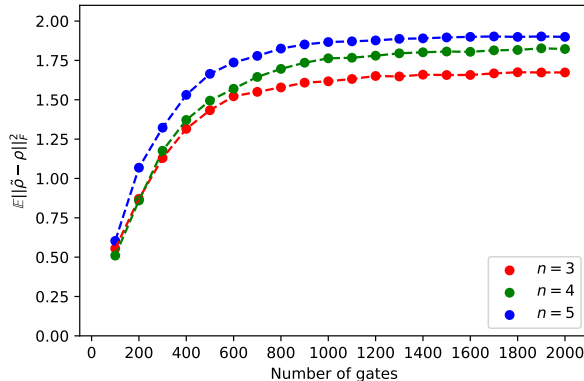
Figure 1. Propagated error for Quantum Fourier Transform (QFT). 3-, 4-, and 5-qubit QFT circuits are simulated repeatedly using the FakeVigo backend provided by IBM Quantum Experience. The propagated error of the circuit is described by $\mathbb{E}\,\|\tilde{\rho} - \rho\|_{\mathrm{F}}^{2}$, where ρ represents the ideal resulting density matrix, and $\tilde{\rho}$ represents the actual resulting density matrix of the noisy circuit. Here the expectation is estimated by the empirical mean of 8192 executions of the truncated circuits.

Theorem 1.1. *Given a quantum circuit with a sequence of single-qubit or double-qubit gates $G_1, \cdots, G_m$ starting with an initial density matrix ρ_0. Each gate G_k is implemented with a probabilistic error P_k with error probability $p_k \in [0, 1)$, or a Kraus error in the form of (3) or (5). Then the expected error propagation is bounded as,*

$$\mathbb{E}\,\|\tilde{\rho}_m - \rho_m\|_{\mathrm{F}}^{2} \le 2(1 - (1 - r)^m),$$

where r is a constant, $0 \le r < 1$, independent of the number of qubits.

In addition to the theoretical bound, we verify our analysis bound using numerical experiments on quantum simulators, including a simulator of IBM Vigo quantum computer. Numerical results for the Kraus and probabilistic models are performed on quantum simulators to demonstrate the tightness of our bounds. Also, numerical examples of QFT with various numbers of qubits are included to verify our analytical results.

The rest paper is organized as follows. In Section 2, two types of error models are included and explained in detail. A formal statement of the linearly growing quantum error bound is given. The refined analysis of the error bounds for Kraus and probabilistic models are given in Section 3 and Section 4, respectively. In Section 4, we also give a bound on the mixed error model, i.e., prove Theorem 1.1. Section 5 shows the numerical experiments verifying our bounds and demonstrates the tightness. Finally, we conclude our paper in Section 6 with a discussion on future work.

2. Quantum Error Models and Linear Error Propagation

The basic unit of quantum computing is quantum bits, or qubits, which is the quantum counterpart of bits in classical computers. A qubit is a two-state quantum-mechanical system. Different from a classical bit, a qubit can be in a coherent superposition of both states simultaneously. Mathematically, the possible states of an n-qubit system form an N-dimensional Hilbert space, where $N = 2^n$, and therefore can be described by an N-dimensional complex vector. Such a state is called a pure state.

When quantum errors are included, the quantum system is no longer isolated from the environment and interacts with the surrounding environment. Then the system cannot be described as a pure state. Instead, it can be described as a probabilistic mixture of a set of pure states. Therefore, density matrices should be used to describe such a mixed state. For an n-qubit quantum system, the state of the system can be described as an $N \times N$ density matrix ρ. A density matrix is a semi-positive definite Hermitian matrix with trace being 1. A useful property is that $\|\rho\|_{\mathrm{F}} \leq 1$, and $\|\rho\|_{\mathrm{F}} = 1$ if and only if ρ represents a pure state.

A quantum algorithm in quantum computing is modeled and compiled into a quantum circuit, where the quantum circuit is composed of a sequence of quantum gates. Basic single-qubit quantum gates include Pauli gates (X, Y, Z), Hadamard gate (H), phase gate (S), etc. Double-qubit gates include controlled not gate $(CNOT)$, controlled Z (CZ), etc. A single-qubit and a double-qubit gate can be described as a two-dimensional and a four-dimensional unitary matrix, respectively. For an n-qubit quantum circuit, a single-qubit operator U acting on the j-th qubit can be described as an N-dimensional unitary matrix admitting a tensor product form $I \otimes \cdots \otimes I \otimes U \otimes I \otimes \cdots \otimes I$, where I is a two-dimensional identity matrix and U appears at the j-th position. Double-qubit operators on n-qubit circuit admit a similar tensor product form with two positions replaced by the 4-dimensional submatrix. Therefore, each gate acting on an n-qubit quantum circuit can be described as a unitary matrix $U \in \mathcal{U}(N)$, where $\mathcal{U}(N)$ denotes the set of all unitary matrices of size N by N. Therefore, applying a quantum gate G on a quantum state ρ leads to a new state $U \rho U^{\dagger}$, where U is the underlying unitary matrix of G.

2.1. **Quantum error models.** There are two widely adopted mathematical models describing quantum errors, namely the probabilistic error model and the Kraus error model. Under the probabilistic error model, after a gate G is applied on some qubits, there is a nonzero probability $p > 0$ that another error operator is applied on the same qubits. The error operator could be X, Y, Z, reset, or other operators. We define the probabilistic error operator as

$$(1) \qquad P(\rho) = \begin{cases} \rho, & \text{with probability } 1 - p \\ \text{another state}, & \text{with probability } p \end{cases}.$$

Throughout this paper, the probabilistic error model is used with a set of error operators, i.e., bit flip (X error), phase flip (Z error), bit-phase flip (Y error), reset error, and depolarizing error.

Under the Kraus error model, after a gate G is applied, a Kraus operator will be applied afterward, where the Kraus operator admits,

$$K(\rho) = V_1 \rho V_1^\dagger + \cdots + V_K \rho V_K^\dagger,$$

for

(2)
$$\sum_{k=1}^{K} V_k^\dagger V_k = I.$$

Here $\{V_k\}_{k=1}^{K}$ are gate G dependent. Two Kraus error examples are amplitude damping and phase damping. Both errors work as $\mathcal{E}(\rho) = V_1 \rho V_1^\dagger + V_2 \rho V_2^\dagger$, with

$$V_1 = \begin{pmatrix} 1 & 0 \\ 0 & \sqrt{1-\gamma} \end{pmatrix}, V_2 = \begin{pmatrix} 0 & \sqrt{\gamma} \\ 0 & 0 \end{pmatrix},$$

for amplitude damping, and

$$V_1 = \begin{pmatrix} 1 & 0 \\ 0 & \sqrt{1-\lambda} \end{pmatrix}, V_2 = \begin{pmatrix} 0 & 0 \\ 0 & \sqrt{\lambda} \end{pmatrix},$$

for phase damping, where γ and λ are parameters in amplitude damping and phase damping, respectively.

The probabilistic error model and Kraus error model appear in quite different forms, but they are deeply related. In fact, the probabilistic error model can be equivalently written in the Kraus format. A few typical examples are included in Appendix A.

As we mentioned earlier, quantum gates are applied to one or two qubits. Both the probabilistic error model and Kraus error model we discuss in this work are associated with quantum gates and are applied to the same qubits after the gate operation. The probabilistic error models on one or two qubits are the same as (1). For Kraus error models, we focus on specific forms for single-qubit and double-qubit systems, which are widely adopted in quantum simulators and cover a wide range of quantum errors. The Kraus error model for single-qubit systems admits,

(3)
$$K_{\text{sq}}(\rho) = V_1 \rho V_1^\dagger + V_2 \rho V_2^\dagger + V_3 \rho V_3^\dagger + V_4 \rho V_4^\dagger,$$

where

(4)
$$V_1 = \begin{pmatrix} a_1 & 0 \\ 0 & b_1 \end{pmatrix}, \quad V_2 = \begin{pmatrix} a_2 & 0 \\ 0 & b_2 \end{pmatrix}, \quad V_3 = \begin{pmatrix} 0 & 0 \\ a_3 & 0 \end{pmatrix}, \quad V_4 = \begin{pmatrix} 0 & b_3 \\ 0 & 0 \end{pmatrix},$$

satisfying $V_1^\dagger V_1 + V_2^\dagger V_2 + V_3^\dagger V_3 + V_4^\dagger V_4 = I$. The equality constraint on V_is is equivalent to

$$a_1^2 + a_2^2 + a_3^2 = 1 \quad \text{and} \quad b_1^2 + b_2^2 + b_3^2 = 1.$$

Without loss of generality, we assume that $\det\left\{\begin{pmatrix} a_1 & a_2 \\ b_1 & b_2 \end{pmatrix}\right\} \neq 0$.

For a double-qubit system, if both qubits have Kraus errors in the form of (3) being

$$K_1(\rho) = V_{11} \rho V_{11}^\dagger + V_{12} \rho V_{12}^\dagger + V_{13} \rho V_{13}^\dagger + V_{14} \rho V_{14}^\dagger,$$
$$K_2(\rho) = V_{21} \rho V_{21}^\dagger + V_{22} \rho V_{22}^\dagger + V_{23} \rho V_{23}^\dagger + V_{24} \rho V_{24}^\dagger,$$

then the effect on the double-qubit system can be written as a Kraus model

$$(5) \qquad K_{\mathrm{dq}}(\rho) = (K_1 \otimes K_2)(\rho) = \sum_{j=1}^{16} V_j \rho V_j^\dagger,$$

where $\rho \in \mathbb{C}^{4\times 4}$ represents the density matrix of the double-qubit systems, and matrices are tensor products $\{V_j\}_{j=1}^{16} = \{V_{1i} \otimes V_{2j}\}_{i,j=1}^4$. The patterns of $\{V_j\}_{j=1}^{16}$ can be found in Appendix B.

The Kraus error models as in (3) and (5) are closed under composition operation, i.e., the composition of two Kraus error models in the form of (3) can be represented as a new Kraus error model, also in the form of (3). Lemma 2.1 and Lemma 2.2 shows the composition properties of single-qubit and double-qubit Kraus error model, respectively.

Lemma 2.1. *Suppose two single-qubit Kraus errors K_1 and K_2 are in the form of (3) with matrices and coefficients being denoted as $\{V_{ji}\}_{i=1}^4$ and $\{a_{ji}, b_{ji}\}_{i=1}^3$ respectively for $j = 1, 2$. We further assume that*

$$(6) \qquad a_{13}^2 + a_{23}^2 \leq 1, \quad b_{13}^2 + b_{23}^2 \leq 1.$$

Then the composition of K_1 and K_2, $K = K_2 \circ K_1$, is another Kraus error in the form of (3).

Lemma 2.2. *Suppose two double-qubit Kraus errors $K_1 = K_{11} \otimes K_{21}$ and $K_2 = K_{12} \otimes K_{22}$ are in the form of (5). We further assume that the parameters for both pairs K_{11}, K_{12}, and K_{21}, K_{22} satisfy (6). Then the composition of K_1 and K_2, $K = K_2 \circ K_1$, is another Kraus error in the form of (5).*

Proofs of Lemma 2.1 and Lemma 2.2 can be found in Appendix C. In Kraus error models as (3) and (5), V_j for $j \geq 2$ terms are viewed as errors, and hence, the parameters a_i and b_i for $i \geq 2$ are close to 0. Thus the assumptions of a_i and b_i are found reasonable in practice.

Other than the gate error models discussed above, the thermal relaxation error model, which describes how errors may occur as time goes by, can also be expressed in either the probabilistic error model or the Kraus error model. Suppose a thermal relaxation channel is parametrized by relaxation time constant T_1, T_2, gate time t, and excited state thermal population p_1. If $T_1 < T_2$, then the thermal relaxation channel can be expressed as a Kraus channel $\mathcal{E}(\rho) = \sum_{j=1}^4 V_j \rho V_j^\dagger$, with

$$V_1 = \begin{pmatrix} 1 - p_1 p_{\mathrm{reset}} & 0 \\ 0 & e^{-t/T_2} \end{pmatrix}, \quad V_2 = \begin{pmatrix} e^{-t/T_2} & 0 \\ 0 & 1 - p_0 p_{\mathrm{reset}} \end{pmatrix},$$

$$V_3 = \begin{pmatrix} 0 & 0 \\ p_0 p_{\mathrm{reset}} & 0 \end{pmatrix}, \quad V_4 = \begin{pmatrix} 0 & p_1 p_{\mathrm{reset}} \\ 0 & 0 \end{pmatrix},$$

where $p_0 = 1 - p_1$ and $p_{\mathrm{reset}} = 1 - e^{-t/T_1}$. If $T_1 > T_2$, then the channel is equivalent to a probabilistic model, with $p_{R0} = p_0 p_{\mathrm{reset}}, p_{R1} = p_1 p_{\mathrm{reset}}, p_Z = \frac{(1 - p_{\mathrm{reset}})}{2}\left(1 - e^{\left(-t(\frac{1}{T_2} - \frac{1}{T_1})\right)}\right)$, and $p_I = 1 - p_{R0} - p_{R1} - p_Z$, where $R0$ and $R1$ represent the reset transformation to $|0\rangle\langle 0|$ and $|1\rangle\langle 1|$, respectively.

In Lemma 2.3, we show that some quantum errors, which are introduced as probabilistic errors, could be represented as Kraus errors as well.

Lemma 2.3. *Assume the probabilities of X error and Y error are equal, i.e., $p_X = p_Y$, then any combination of X error, Y error, Z error, reset to $|0\rangle\langle 0|$, reset to $|1\rangle\langle 1|$, and depolarizing error can be written as a Kraus error in the form of* (3).

Proof of Lemma 2.3 can be found in Appendix C.

All mentioned errors can be described by either the Kraus error model (3) or the probabilistic error model. We summarize the error models and various types of errors in Table 1.

Error type	Probabilistic error model	Kraus error model (3)
X	✓	✗
Y	✓	✗
Z	✓	✓
Reset to $|0\rangle\langle 0|$	✓	✓
Reset to $|0\rangle\langle 0|$	✓	✓
Depolarizing	✓	✓
Amplitude damping	✗	✓
Phase damping	✗	✓
Thermal relaxation	✗	✓
Combination	✗	Conditioned

Table 1. The errors each error model can describe respectively. The combination of errors can be described by the Kraus error model in the form of (3) under the condition that the probabilities of X error and Y error are equal, i.e. $p_X = p_Y$.

2.2. **Linear growing error analysis.** We consider a quantum circuit with a sequence of m quantum gates $G_1, \cdots, G_m$ and their corresponding unitary matrices being $U_1, \cdots, U_m$. We further denote ρ_0 as the initial density matrix, and ρ_k as the error-free density matrix after k gates have been implemented, i.e.,

$$\rho_k = U_k \cdots U_1 \rho_0 U_1^\dagger \cdots U_k^\dagger. \tag{7}$$

The actual density matrix with quantum error after k gates is denoted as $\tilde{\rho}_k$, i.e.,

$$\tilde{\rho}_0 = \rho_0,$$
$$\tilde{\rho}_1 = E_1 \left(U_1 \tilde{\rho}_0 U_1^\dagger \right),$$
$$\cdots$$
$$\tilde{\rho}_m = E_m \left(U_m \tilde{\rho}_{m-1} U_m^\dagger \right),$$

where E_i is either a probabilistic error operator P, a Kraus error operator K, or their composition. Notice that $\tilde{\rho}_k$ has randomness if there are probabilistic errors.

A linearly growing bound for both Kraus error and probabilistic error can be proved easily. We first give Lemma 2.4 and Lemma 2.5 for Kraus error model and probabilistic error model respectively. Then, Lemma 2.6 gives the linear growing bound for mixed errors.

Lemma 2.4. *Given a quantum circuit with a sequence of quantum gates* $G_1, \cdots, G_m$ *starting with an initial density matrix* ρ_0. *Each gate* G_k *is implemented with a Kraus error* K_k. *Suppose there is a constant* $\gamma_1 > 0$ *such that*

$$(8) \qquad \qquad \|K_k(\rho) - \rho\|_{\mathrm{F}} \leq \gamma_1,$$

for any density matrix ρ *and* $k = 1, \cdots, m$. *Then the error of density matrix grows at most linearly,*

$$(9) \qquad \qquad \|\tilde{\rho}_m - \rho_m\|_{\mathrm{F}} \leq \gamma_1 m.$$

Notice that Lemma 2.4 shows the error growing for the general Kraus error model. A probabilistic error P with probability p can be expressed as a general Kraus error,

$$(10) \qquad \qquad P(\rho) = p\rho + (1-p)R\rho R^{\dagger} = V_1 \rho V_1^{\dagger} + V_2 \rho V_2^{\dagger},$$

where $V_1 = \sqrt{p}I$, $V_2 = \sqrt{1-p}R$, and unitary R maps ρ to another state. Therefore, we have the following results, which could be viewed as corollaries of Lemma 2.4.

Lemma 2.5. *Given a quantum circuit with a sequence of quantum gates* $G_1, \cdots, G_m$ *starting with an initial density matrix* ρ_0. *Each gate* G_k *is implemented with a probabilistic error* P_k *with probability* $0 < p_k \leq 1$. *Then there is a constant* $\gamma_2 > 0$ *such that*

$$(11) \qquad \qquad \mathbb{E} \|\tilde{\rho}_m - \rho_m\|_{\mathrm{F}} \leq \gamma_2 m.$$

Lemma 2.6. *Given a quantum circuit with a sequence of quantum gates* $G_1, \cdots, G_m$ *starting with an initial density matrix* ρ_0. *Each gate* G_k *is implemented with either a probabilistic error with probability* $0 < p_k \leq 1$, *a Kraus error satisfying* (8), *or a mix of both. Then there is a constant* $\gamma \geq 0$ *independent of the number of qubits, such that*

$$\mathbb{E} \|\tilde{\rho}_m - \rho_m\|_{\mathrm{F}} \leq \gamma m.$$

The proofs of Lemma 2.4 and Lemma 2.5 are given in Appendix D. Lemma 2.6 could be viewed as a simple composition of Lemma 2.4 and Lemma 2.5, and is stated without detailed proof.

However, a linear growing upper bound does not agree well with experimental results in Figure 1. A simple inequality for the Frobenius norm of the difference between two density matrices indicates that the quantum error should be upper bounded by a constant, i.e.,

$$(12) \qquad \qquad \|\tilde{\rho} - \rho\|_{\mathrm{F}}^2 = \|\tilde{\rho}\|_{\mathrm{F}}^2 + \|\rho\|_{\mathrm{F}}^2 - 2\mathrm{tr}\,(\tilde{\rho}\rho) \leq 2,$$

for any density matrices $\tilde{\rho}$ and ρ, where the last inequality is based on the fact that the product of two semi-definite matrices has non-negative trace [12]. Therefore, the linear growing bound cannot characterize the error propagates as the number of gates increases. A tighter bound for quantum error propagations is desired.

3. Analysis of Kraus Error Propagation

In this section, we focus on the analysis of quantum error propagation for quantum circuits with Kraus error as in the form of (3) and (5) only. The setting could be fairly similar to that in Lemma 2.4. But conclusions are dramatically different. In this section, we show that the error propagation would scale as $1 - (1-q)^m$, where m is the depth and q is a constant, $0 \leq q < 1$, depending on Kraus error parameters. The major result of this section is given in Theorem 3.1. Lemma 3.1, Lemma 3.2, and Lemma 3.3 are proposed and proved to facilitate the proof of Theorem 3.1.

Theorem 3.1. *Given a quantum circuit with a sequence of single-qubit or double-qubit gates $G_1, \cdots, G_m$ starting with an initial density matrix ρ_0. Each gate G_k is implemented with a Kraus error K_k as in form (3) or (5). Then the error propagation is bounded as,*

$$\|\tilde{\rho}_m - \rho_m\|_{\mathrm{F}}^2 \leq 2(1 - (1-q)^m), \tag{13}$$

where q is a constant, $0 \leq q < 1$, independent of the number of qubits.

Before giving precise proof of Theorem 3.1, we first sketch the key ideas therein. The basic idea is to find a constant $q \in [0, 1)$, for q as small as possible, such that

$$\|\tilde{\rho}_k - \rho_k\|_{\mathrm{F}}^2 \leq (1-q) \|\tilde{\rho}_{k-1} - \rho_{k-1}\|_{\mathrm{F}}^2 + 2q, \tag{14}$$

where $\tilde{\rho}_k$ and ρ_k are noisy and noiseless density matrix after acting k gates, respectively. Then, we could recursively apply (14), and obtain,

$$
\begin{aligned}
\|\tilde{\rho}_m - \rho_m\|_{\mathrm{F}}^2 &\leq (1-q) \|\tilde{\rho}_{m-1} - \rho_{m-1}\|_{\mathrm{F}}^2 + 2q \\
&\leq (1-q) \left((1-q) \|\tilde{\rho}_{m-2} - \rho_{m-2}\|_{\mathrm{F}}^2 + 2q \right) + 2q \\
&\leq \cdots \\
&\leq 2q \left(1 + (1-q) + \cdots + (1-q)^{m-1} \right) \\
&= 2(1 - (1-q)^m),
\end{aligned}
\tag{15}
$$

which is the conclusion of Theorem 3.1. Substituting the gate and quantum error action in the matrix form, (14) is equivalent to

$$
\begin{aligned}
\left\| K_k \left(U_k \tilde{\rho}_{k-1} U_k^\dagger \right) - U_k \rho_{k-1} U_k^\dagger \right\|_{\mathrm{F}}^2 &\leq (1-q) \|\tilde{\rho}_{k-1} - \rho_{k-1}\|_{\mathrm{F}}^2 + 2q \\
&= (1-q) \left\| U_k \tilde{\rho}_{k-1} U_k^\dagger - U_k \rho_{k-1} U_k^\dagger \right\|_{\mathrm{F}}^2 + 2q.
\end{aligned}
\tag{16}
$$

Denoting $\tilde{\rho} = U_k \tilde{\rho}_{k-1} U_k^\dagger$ and $\rho = U_k \rho_{k-1} U_k^\dagger$, (16) can, then, be written as

$$\|K_k(\tilde{\rho}) - \rho\|_{\mathrm{F}}^2 \leq (1-q) \|\tilde{\rho} - \rho\|_{\mathrm{F}}^2 + 2q. \tag{17}$$

We define a function F of Kraus error K, density matrices $\tilde{\rho}$ and ρ as

$$F(K; \tilde{\rho}, \rho) = \begin{cases} \frac{\|K(\tilde{\rho}) - \rho\|_{\mathrm{F}}^2 - \|\tilde{\rho} - \rho\|_{\mathrm{F}}^2}{2 - \|\tilde{\rho} - \rho\|_{\mathrm{F}}^2}, & \|\tilde{\rho} - \rho\|_{\mathrm{F}}^2 < 2 \\ \lim_{\tilde{\rho}' \to \tilde{\rho}, \rho' \to \rho} F(K; \tilde{\rho}', \rho'), & \|\tilde{\rho} - \rho\|_{\mathrm{F}}^2 = 2 \end{cases}. \tag{18}$$

Then, finding a constant q, as small as possible, satisfying (17) could be addressed by finding an upper bound of $F(K; \tilde{\rho}, \rho)$, i.e.,

$$(19) \qquad q = \sup_{\tilde{\rho}, \rho} F(K; \tilde{\rho}, \rho).$$

Since $\|K(\tilde{\rho}) - \rho\|_{\mathrm{F}}^2 \leq 2$ (see (26)), it always holds $F(K; \tilde{\rho}, \rho) \leq 1$. However, this is not sufficient for us to estimate a tighter upper bound for F. To achieve our goal, we need $F(K; \tilde{\rho}, \rho)$ to be strictly less than 1 for all $\tilde{\rho}$ and ρ, which is guaranteed by the following lemmas.

Lemma 3.1. *Suppose K_{sq} is a single-qubit Kraus operator in the form of* (3). *Then there exist a constant $\delta > 0$ independent of n, such that*

$$\|K_{sq}(\rho)\|_{\mathrm{F}}^2 \leq 1 - \delta$$

for any n-qubit density matrix $\rho \in \mathbb{C}^{N \times N}$.

Lemma 3.2. *Suppose K_{dq} is a double-qubit Kraus operator in the form of* (5). *Then there is a constant $\delta > 0$ independent of n, such that*

$$\|K_{dq}(\rho)\|_{\mathrm{F}}^2 \leq 1 - \delta$$

for any n-qubit density matrix $\rho \in \mathbb{C}^{N \times N}$.

In both Lemma 3.1 and Lemma 3.2, we do not have explicit expressions for δ. We only prove the existence of δ satisfying $\delta > 0$. Both proofs of Lemma 3.1 and Lemma 3.2 obey the following flow. First, by triangle inequality, it can be proved that $\|K(\rho)\|_{\mathrm{F}} \leq 1$. Then we illustrate that the equality condition cannot hold for K_{sq} and K_{dq}, i.e., $\|K(\rho)\|_{\mathrm{F}} < 1$ for both K_{sq} and K_{dq}. Moreover, since K is a continuous function of density matrix ρ, which is defined on a compact set, the maximum of this function can be achieved. Therefore, the upper bound of $\|K(\rho)\|_{\mathrm{F}}$ is strictly less than 1, for both K_{sq} and K_{dq}. Appendix F proves Lemma 3.1 and Lemma 3.2 in detail.

With Lemma 3.1 and Lemma 3.2, we then have the following lemma.

Lemma 3.3. *Suppose K is a single-qubit Kraus operator in the form of* (3) *or a double-qubit Kraus operator in the form of* (5). *There is a constant $0 \leq q < 1$, such that*

$$(20) \qquad F(K; \tilde{\rho}, \rho) \leq q,$$

for any density matrices $\tilde{\rho}$ and ρ.

Proof. According to Lemma 3.1 or Lemma 3.2, there is a constant $\delta > 0$ such that $\|K(\rho)\|_{\mathrm{F}}^2 \leq 1 - \delta$ for any density matrix ρ. Therefore, it holds

$$\|K(\tilde{\rho}) - \rho\|_{\mathrm{F}}^2 = \|K(\tilde{\rho})\|_{\mathrm{F}}^2 + \|\rho\|_{\mathrm{F}}^2 - 2\mathrm{tr}\left(K(\tilde{\rho})\rho\right) \leq 2 - \delta,$$

where the second inequality adopts the positivity of $K(\tilde{\rho})$ and Ruhe's trace inequality. Thus, for any density matrices $\tilde{\rho}$ and ρ such that $\|\tilde{\rho} - \rho\|_{\mathrm{F}}^2 \neq 2$, it holds

$$F(K; \tilde{\rho}, \rho) = \frac{\|K(\tilde{\rho}) - \rho\|_{\mathrm{F}}^2 - \|\tilde{\rho} - \rho\|_{\mathrm{F}}^2}{2 - \|\tilde{\rho} - \rho\|_{\mathrm{F}}^2} \leq \frac{2 - \delta}{2}.$$

When $\|\tilde{\rho} - \rho\|_{\mathrm{F}}^2 = 2$, it holds

$$F(K; \tilde{\rho}, \rho) = \lim_{\tilde{\rho}' \to \tilde{\rho}, \rho' \to \rho} F(K; \tilde{\rho}', \rho') \leq \frac{2 - \delta}{2}.$$

Setting $q = \frac{2-\delta}{2} < 1$, we have (20).

<div align="right">□</div>

Finally, we prove Theorem 3.1 using Lemma 3.3.

Proof of Theorem 3.1. For each Kraus operator K_k, according to Lemma 3.3, there is a constant $0 \leq q_k < 1$ such that $F(K_k; \tilde{\rho}, \rho) \leq q_k$, for any density matrices $\tilde{\rho}$ and ρ. Let $q = \max\{q_1, \cdots, q_m\} < 1$. Following the derivations from (14) to (19), (13) is proved.

<div align="right">□</div>

4. Analysis of Mixed Error Propagation

Following the flow in Section 2, we first prove the expected error propagation for a quantum circuit with only probabilistic errors, as in Theorem 4.1. Then, we combine the results of Theorem 3.1 and Theorem 4.1 to show that the error propagation of a quantum circuit with both Kraus errors and probabilistic errors can be bounded by $2(1 - (1 - r)^m)$, where m is the number of gates and r is a constant in $[0, 1)$ independent of m. The combined result is known as the error propagation of mixed error models, which is formally stated in Theorem 1.1.

4.1. **Analysis of Probabilistic Error Propagation.** For a quantum circuit with only probabilistic errors, we could write the expected error propagation into two parts: at least one error occurs and no error occurs. Since the difference between any two density matrices is bounded by a constant, the "at least one error occurs" part is bounded by its probability, which scales as $(1 - (1 - p)^m)$. The "no error occurs" part does not contribute to the error propagation and is omitted directly. Put two together, we obtain the Theorem 4.1 for the quantum circuit with probabilistic error only.

Theorem 4.1. *Given a quantum circuit with a sequence of single-qubit or double-qubit gates $G_1, \cdots, G_m$ starting with an initial density matrix ρ_0. Each gate G_k is implemented with a probabilistic error P_k with error probability $p_k \in [0, 1)$. Then the expected error propagation is bounded as,*

$$\mathbb{E} \|\tilde{\rho}_m - \rho_m\|_{\mathrm{F}}^2 \leq 2(1 - (1 - p)^m),$$

where p is a constant, $0 \leq p < 1$, independent of the number of qubits.

Proof. If at least one error occurs in applying $G_1, \cdots, G_m$, then we use (12) to bound $\|\tilde{\rho}_m - \rho_m\|_{\mathrm{F}}^2 \leq 2$. Denote $p = \max_{1 \leq k \leq m} p_k$. Then expected error propagation can be bounded as,

$$\mathbb{E} \|\tilde{\rho}_m - \rho_m\|_{\mathrm{F}}^2 \leq 2 \cdot \mathbb{P}(\text{at least one error occurs}) + \|\rho_m - \rho_m\|_{\mathrm{F}}^2 \cdot \mathbb{P}(\text{no error})$$

$$= 2 \left(1 - \prod_{k=1}^m (1 - p_k)\right) \leq 2 \left(1 - (1 - p)^m\right),$$

where the probability of no error is $\prod_{k=1}^{m}(1-p_k)$, and that at least one error occurs is $1 - \prod_{k=1}^{m}(1-p_k)$.

<div align="right">□</div>

4.2. **Proof of Mixed Error Propagation.** Combining Theorem 3.1 and Theorem 4.1 together, we can then prove Theorem 1.1, which characterizes the expected error propagation of mixed error. The proof flow can also be adapted to prove Lemma 2.6.

Proof of Theorem 1.1. Suppose there are m_K gates with Kraus errors and m_P gates with probabilistic errors, with error probability being $p_1, \cdots, p_{m_P}$. If no probabilistic error occurs, of which the probability is $\mathbb{P}(\text{no error}) = \prod_{k=1}^{m_P}(1-p_k)$, then the system is reduced to a circuit with only Kraus errors. By Theorem 3.1, there is a constant $q \in [0,1)$ such that,

$$\|\tilde{\rho}_m - \rho_m\|_{\mathrm{F}}^2 \le 2\left(1 - (1-q)^{m_K}\right).$$

We then adopt the decomposition as in the proof of Theorem 4.1. The expected error propagation is bounded as,

$$\mathbb{E}\|\tilde{\rho}_m - \rho_m\|_{\mathrm{F}}^2 \le 2 \cdot \mathbb{P}(\text{at least one error occurs}) + \|\tilde{\rho}_m - \rho_m\|_{\mathrm{F}}^2 \cdot \mathbb{P}(\text{no error})$$

$$\le 2\left(1 - \prod_{k=1}^{m_P}(1-p_k)\right) + 2\left(1 - (1-q)^{m_K}\right)\prod_{k=1}^{m_P}(1-p_k)$$

$$= 2\left(1 - (1-q)^{m_K}\prod_{k=1}^{m_P}(1-p_k)\right) \le 2\left(1 - (1-r)^{m}\right),$$

where $r = \max\{p_1, \cdots, p_{m_P}, q\} < 1$.

<div align="right">□</div>

5. NUMERICAL EXPERIMENTS

In this section, we simulate quantum circuits using the quantum device backends provided by IBM Quantum Experience. In these quantum device backends, both the Kraus error model and the probabilistic error model are adopted to represent different types of quantum errors. Hence, these backend simulators are well characterized by our mixed error models as in Theorem 1.1. We also simulate quantum circuits to validate Theorem 3.1 for the Kraus errors and Theorem 4.1 for probabilistic errors separately with each of these error models.

Kraus Error. We first simulate a single-qubit circuit consisting of identity gates with only Kraus error in the form of (3) with parameters being $a_2 = b_2 = 0.001$, $a_3 = 0.08$, $b_3 = 0.008$, $a_1 = \sqrt{1 - a_2^2 - a_3^2} \approx 0.9968$, and $b_1 = \sqrt{1 - b_2^2 - b_3^2} = 0.99997$. We simulate the setup with various circuit depths from 100 to 2000. The Frobenius norm of the density matrix difference is measured every 100 gate, demonstrating the error propagation. We plot both the empirical error propagation as well as the upper bound given in Theorem 4.1 in Figure 2. The constant q in Theorem 4.1 is not explicitly given. For the above Kraus error model setup, we estimate q by random sampling 10^8 pairs of density matrices $\tilde{\rho}$ and ρ and find the maximum value of $F(K; \tilde{\rho}, \rho)$. The matrices are generated by $R\Lambda R^T$, where R is a rotation matrix with uniformly

sampled rotation angle, and Λ is uniformly sampled positive semi-definite diagonal matrix with trace being 1. The estimated constant q is 5.620×10^{-3}. The result is shown in Figure 2.
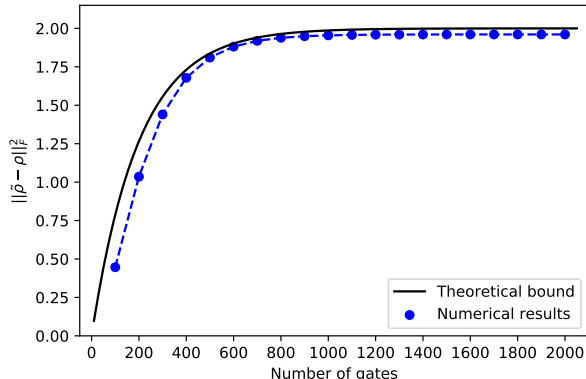
Figure 2. Numerical experiments for identity circuit with Kraus errors only. A quantum circuit consisting of single-qubit identity gates is simulated using 'qasm' backend. Each gate is implemented with a Kraus error. The resulting density matrix is measured for every 100 gate.

Theorem 3.1 provides an upper bound for the error propagation. As shown in Figure 2, with the estimated q, the numerical errors are bounded by our theoretical bound, and the two curves are fairly close to each other. Since our result is a worst-case upper bound, from Figure 2, we are confident that our analysis provides a fairly tight upper bound.

Probabilistic Error. We then simulate a single-qubit circuit consisting of identity gates with only probabilistic error using 'qasm' backend. For each gate, there is a probability $p = 0.005$ for reset-to-$|1\rangle\langle1|$ error. Similarly, we simulate the setup with various circuit depths from 100 to 2000. The Frobenius norm of the density matrix difference is measured every 100 gate, demonstrating the error propagation. Each circuit is repeatedly executed 8192 times to approximate the expectation value of the error. We plot both the empirical expected error propagation as well as the upper bound given in Theorem 4.1 in Figure 3.

Our analysis results in Theorem 4.1 provides an upper bound for the error expectation value, which is not necessarily an upper bound for the sample mean of the error. While, as shown in Figure 3, the numerical errors are tightly bounded by our theoretical bound.

Mixed Error. Finally, we simulate a multi-qubit circuit with both Kraus error and probabilistic errors. The base circuit is chosen to be the same as that in Figure 1, i.e., 3-, 4-, and 5-qubit QFT circuits. The quantum simulator used in this case is the FakeVigo backend, which is configured to simulate IBM Vigo quantum computer. For the purpose of verifying our theoretical bound, we turn off the readout error and measurement error, and only keep the gate errors. The constant in Theorem 4.1 is read from the configuration, $p = 1.076 \times 10^{-2}$. The constants for various Kraus errors in Theorem 3.1 are estimated separately in the same way as that in the Kraus error numerical part, and the overall constant is found to be $q \approx 4.769 \times 10^{-3}$.
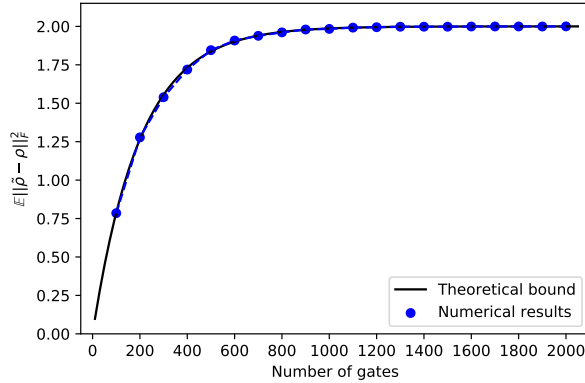
Figure 3. Numerical experiments for single-qubit identity circuit with probabilistic errors only. Each gate is implemented with a reset-to-$|1\rangle\langle1|$ error with probability $p = 0.005$. Each circuit is repeatedly executed for 8192 to approximate the error expectation value.

Thus, the constant r in Theorem 1.1 is set to be $r = \max\{p, q\} = 1.076 \times 10^{-2}$. Since the resulting upper bound in Theorem 1.1 is independent of the number of qubits, we plot the theoretical upper bound for all three multi-qubit circuits as the black curve in Figure 4.
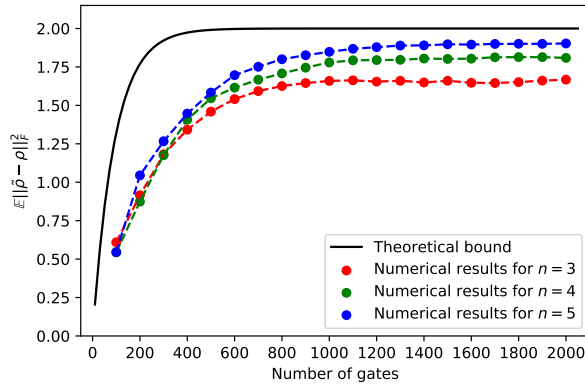
Figure 4. Numerical experiments for repeated 3, 4, and 5-qubit QFT circuits on FakeVigo backend with only gate errors. Each circuit is repeatedly executed for 8192 to approximate the error expectation value.

According to Figure 4, we find that our analysis result in Theorem 1.1 is indeed an upper bound for all three quantum circuits on 3-, 4-, and 5-qubit systems. Vigo is a 5-qubit quantum computer. Different qubits in Vigo actually have different error profiles. If we bind the quantum circuit to specific qubits and estimate the constant separately, we could have three different theoretical upper bounds. In this experiment, we simply estimate the constant for all 5 qubits

together and obtain an upper bound for all quantum circuits on Vigo. As we observe from Figure 4, quantum circuits with a larger number of qubits lead to larger errors. Further, in the current quantum computers, even for quantum computers with a small number of qubits, the error quickly grows to a non-negligible level. Quantum circuits with tens to hundreds of depths would be the limit on Vigo. For quantum computers with a larger number of quantum qubits, numerically simulating the density matrix error results is not possible due to the exponentially increasing size of the density matrix. However, our theoretical upper bound could still be calculated and provide a fairly good estimation on the error growth.

6. Conclusion

Quantum computing is becoming a promising tool for computational tasks. While the quantum hardware is not perfect and is expected to bear with large noise for a long time. The performance of quantum computers nowadays is limited by quantum gate errors and sampling errors. Therefore, we aim to characterize the quantum error that grows with the number of gates in a quantum circuit.

In this work, we first use traditional numerical analysis methods to prove that quantum error grows linearly with the depth of a circuit. However, a simple calculation of the density matrices suggests that the error could not grow linearly but hit a plateau towards the end instead. We, therefore, provided a more carefully analyzed upper bound that better characterizes the growth of the quantum error with the depth of a circuit. To be more specific, we analyzed the probabilistic error model, the Kraus error model, and the mix of both. For all three cases, the error grows as $\sim (1 - (1 - c)^m)$, where c is a constant independent of qubit number and circuit depth (c is different for different error models), and m is the number of quantum gates in the circuit. Finally, we did numerical experiments on the simulator of the Vigo quantum computer provided by IBM Quantum Experience. Numerical results for identity quantum circuits and QFT circuits suggested that our theoretical bound is tight. The errors of QFT circuits are well controlled by our bound.

An immediate future direction is to explore different metrics of the quantum error propagations. We know that all metrics in a finite-dimensional Hilbert space are equivalent. Hence, our results could be directly extended to other metrics with an extra dimension dependent constant. A more careful analysis could reduce such a constant. Another future direction is to obtain a qualititive estimation of the constant q, p, and r in Theorem 3.1, Theorem 4.1, and Theorem 1.1 respectively.

References

[1] Joel Bierman, Yingzhou Li, and Jianfeng Lu, *Quantum Orbital Minimization Method for Excited States Calculation on Quantum Computer*, arXiv e-prints (January 2022), arXiv:2201.07963, available at `2201.07963`.

[2] A. R. Calderbank, E. M. Rains, P. W. Shor, and N. J. A. Sloane, *Quantum error correction and orthogonal geometry*, Phys. Rev. Lett. **78** (1997Jan), 405–408.

[3] A. R. Calderbank and Peter W. Shor, *Good quantum error-correcting codes exist*, Phys. Rev. A **54** (1996Aug), 1098–1105.

[4] A.R. Calderbank, E.M. Rains, P.M. Shor, and N.J.A. Sloane, *Quantum error correction via codes over gf(4)*, IEEE Transactions on Information Theory **44** (1998), no. 4, 1369–1387.

[5] Abhinav Deshpande, Pradeep Niroula, Oles Shtanko, Alexey V. Gorshkov, Bill Fefferman, and Michael J. Gullans, *Tight bounds on the convergence of noisy random circuits to the uniform distribution*, 2021. arXiv:2112.00716.

[6] David Deutsch and Richard Jozsa, *Rapid solution of problems by quantum computation*, Proceedings of the Royal Society of London. Series A: Mathematical and Physical Sciences **439** (1992), no. 1907, 553–558.

[7] Stuart Flannigan, Natalie Pearson, Guang Hao Low, Anton S. Buyskikh, Immanuel Bloch, Peter Zoller, Matthias Troyer, and Andrew J. Daley, *Propagation of errors and quantitative quantum simulation with quantum advantage*, 2022. arXiv:2204.13644.

[8] Paul Gallot, Anca Muscholl, Gabriele Puppis, and Sylvain Salvati, *On the decomposition of finite-valued streaming string transducers*, Leibniz International Proceedings in Informatics **66** (2017), 14.

[9] Daniel Gottesman, *Class of quantum error-correcting codes saturating the quantum hamming bound*, Phys. Rev. A **54** (1996Sep), 1862–1868.

[10] Lov K Grover, *A fast quantum mechanical algorithm for database search*, Proceedings of the twenty-eighth annual acm symposium on theory of computing, 1996, pp. 212–219.

[11] Alexander Müller-Hermes, Daniel Stilck França, and Michael M. Wolf, *Relative entropy convergence for depolarizing channels*, Journal of Mathematical Physics **57** (2016), no. 2, 022202.

[12] Axel Ruhe, *Perturbation bounds for means of eigenvalues and invariant subspaces*, BIT Numerical Mathematics **10** (1970), no. 3, 343–354.

[13] Kunal Sharma, Sumeet Khatri, M Cerezo, and Patrick J Coles, *Noise resilience of variational quantum compiling*, New Journal of Physics **22** (2020apr), no. 4, 043006.

[14] Peter W Shor, *Algorithms for quantum computation: discrete logarithms and factoring*, Proceedings 35th annual symposium on foundations of computer science, 1994, pp. 124–134.

[15] Peter W. Shor, *Scheme for reducing decoherence in quantum computer memory*, Phys. Rev. A **52** (1995Oct), R2493–R2496.

[16] Daniel R Simon, *On the power of quantum computation*, SIAM journal on computing **26** (1997), no. 5, 1474–1483.

[17] Andrew Steane, *Multiple-particle interference and quantum error correction*, Proceedings of the Royal Society of London. Series A: Mathematical, Physical and Engineering Sciences **452** (1996), no. 1954, 2551–2577, available at `https://royalsocietypublishing.org/doi/pdf/10.1098/rspa.1996.0136`.

[18] Jinfeng Zeng, Zipeng Wu, Chenfeng Cao, Chao Zhang, Shi-Yao Hou, Pengxiang Xu, and Bei Zeng, *Simulating noisy variational quantum eigensolver with local noise models*, Quantum Engineering **3** (2021), no. 4, e77, available at `https://onlinelibrary.wiley.com/doi/pdf/10.1002/que2.77`.

Appendix Appendix A. Probabilistic error model in Kraus form

Kraus formulations of typical probabilistic errors are listed below.

- Bit flip with probability p_X:

$$V_1 = \sqrt{p_X}I = \sqrt{p_X}\begin{pmatrix} 1 & 0 \\ 0 & 1 \end{pmatrix}, V_2 = \sqrt{1-p_X}X = \sqrt{1-p_X}\begin{pmatrix} 0 & 1 \\ 1 & 0 \end{pmatrix}.$$

- Phase flip with probability p_Z:

$$V_1 = \sqrt{p_Z}I = \sqrt{p_Z}\begin{pmatrix} 1 & 0 \\ 0 & 1 \end{pmatrix}, V_2 = \sqrt{1-p_Z}Z = \sqrt{1-p_Z}\begin{pmatrix} 1 & 0 \\ 0 & -1 \end{pmatrix}.$$

- Bit-phase flip with probability p_Y:

$$V_1 = \sqrt{p_Y}\, I = \sqrt{p_Y}\begin{pmatrix} 1 & 0 \\ 0 & 1 \end{pmatrix}, V_2 = \sqrt{1-p_Y}\, Y = \sqrt{1-p_Y}\begin{pmatrix} 0 & -\imath \\ \imath & 0 \end{pmatrix}.$$

- Reset to $|0\rangle\langle 0|$ with probability p_{R0}:

$$V_1 = \sqrt{p_{R0}}\begin{pmatrix} 1 & 0 \\ 0 & 1 \end{pmatrix}, V_2 = \sqrt{1-p_{R0}}\begin{pmatrix} 1 & 0 \\ 0 & 0 \end{pmatrix}, V_3 = \sqrt{1-p_{R0}}\begin{pmatrix} 0 & 1 \\ 0 & 0 \end{pmatrix}.$$

- Reset to $|1\rangle\langle 1|$ with probability p_{R1}:

$$V_1 = \sqrt{p_{R1}}\begin{pmatrix} 1 & 0 \\ 0 & 1 \end{pmatrix}, V_2 = \sqrt{1-p_{R1}}\begin{pmatrix} 1 & 0 \\ 0 & 0 \end{pmatrix}, V_3 = \sqrt{1-p_{R1}}\begin{pmatrix} 0 & 0 \\ 1 & 0 \end{pmatrix}.$$

- Depolarizing with probability p_D:

$$V_1 = \sqrt{\frac{1-3p_D}{4}}\, I, V_2 = \frac{\sqrt{p_D}}{2} X, V_3 = \frac{\sqrt{p_D}}{2} Y, V_4 = \frac{\sqrt{p_D}}{2} Z.$$

Appendix Appendix B. Double-qubit Kraus error model

The detailed expressions of V_js in (5) are of forms,

$$V_1 = \begin{pmatrix} a_1 & 0 & 0 & 0 \\ 0 & b_1 & 0 & 0 \\ 0 & 0 & c_1 & 0 \\ 0 & 0 & 0 & d_1 \end{pmatrix}, \quad V_2 = \begin{pmatrix} a_2 & 0 & 0 & 0 \\ 0 & b_2 & 0 & 0 \\ 0 & 0 & c_2 & 0 \\ 0 & 0 & 0 & d_2 \end{pmatrix}, \quad V_3 = \begin{pmatrix} a_3 & 0 & 0 & 0 \\ 0 & b_3 & 0 & 0 \\ 0 & 0 & c_3 & 0 \\ 0 & 0 & 0 & d_3 \end{pmatrix},$$

$$V_4 = \begin{pmatrix} a_4 & 0 & 0 & 0 \\ 0 & b_4 & 0 & 0 \\ 0 & 0 & c_4 & 0 \\ 0 & 0 & 0 & d_4 \end{pmatrix}, \quad V_5 = \begin{pmatrix} 0 & 0 & 0 & 0 \\ 0 & 0 & 0 & 0 \\ a_5 & 0 & 0 & 0 \\ 0 & b_5 & 0 & 0 \end{pmatrix}, \quad V_6 = \begin{pmatrix} 0 & 0 & 0 & 0 \\ 0 & 0 & 0 & 0 \\ a_6 & 0 & 0 & 0 \\ 0 & b_6 & 0 & 0 \end{pmatrix},$$

$$V_7 = \begin{pmatrix} 0 & 0 & 0 & 0 \\ a_7 & 0 & 0 & 0 \\ 0 & 0 & 0 & 0 \\ 0 & 0 & c_7 & 0 \end{pmatrix}, \quad V_8 = \begin{pmatrix} 0 & 0 & 0 & 0 \\ a_8 & 0 & 0 & 0 \\ 0 & 0 & 0 & 0 \\ 0 & 0 & c_8 & 0 \end{pmatrix}, \quad V_9 = \begin{pmatrix} 0 & b_7 & 0 & 0 \\ 0 & 0 & 0 & 0 \\ 0 & 0 & 0 & d_7 \\ 0 & 0 & 0 & 0 \end{pmatrix},$$

$$V_{10} = \begin{pmatrix} 0 & b_8 & 0 & 0 \\ 0 & 0 & 0 & 0 \\ 0 & 0 & 0 & d_8 \\ 0 & 0 & 0 & 0 \end{pmatrix}, \quad V_{11} = \begin{pmatrix} 0 & 0 & c_5 & 0 \\ 0 & 0 & 0 & d_5 \\ 0 & 0 & 0 & 0 \\ 0 & 0 & 0 & 0 \end{pmatrix}, \quad V_{12} = \begin{pmatrix} 0 & 0 & c_6 & 0 \\ 0 & 0 & 0 & d_6 \\ 0 & 0 & 0 & 0 \\ 0 & 0 & 0 & 0 \end{pmatrix},$$

$$V_{13} = \begin{pmatrix} 0 & 0 & 0 & 0 \\ 0 & 0 & 0 & 0 \\ 0 & 0 & 0 & 0 \\ a_9 & 0 & 0 & 0 \end{pmatrix}, \quad V_{14} = \begin{pmatrix} 0 & 0 & 0 & 0 \\ 0 & 0 & 0 & 0 \\ 0 & b_9 & 0 & 0 \\ 0 & 0 & 0 & 0 \end{pmatrix}, \quad V_{15} = \begin{pmatrix} 0 & 0 & 0 & 0 \\ 0 & 0 & c_9 & 0 \\ 0 & 0 & 0 & 0 \\ 0 & 0 & 0 & 0 \end{pmatrix},$$

$$V_{16} = \begin{pmatrix} 0 & 0 & 0 & d_9 \\ 0 & 0 & 0 & 0 \\ 0 & 0 & 0 & 0 \\ 0 & 0 & 0 & 0 \end{pmatrix}$$

The matrices V_j obey normalization condition (2), which is equivalent to

$$\sum_{j=1}^{9} a_j^2 = 1, \quad \sum_{j=1}^{9} b_j^2 = 1, \quad \sum_{j=1}^{9} c_j^2 = 1, \quad \sum_{j=1}^{9} d_j^2 = 1.$$

Similar to the single-qubit Kraus error model, V_1 is close to an identity matrix, while others are close to zero matrices, i.e., a_1, b_1, c_1, d_1 are close to 1, and other parameters are close to 0. Also, the parameters a_j, b_j, c_j, d_j in (B) admits,

$$\det\left\{ \begin{pmatrix} a_1 & a_2 & a_3 & a_4 \\ b_1 & b_2 & b_3 & b_4 \\ c_1 & c_2 & c_3 & c_4 \\ d_1 & d_2 & d_3 & d_4 \end{pmatrix} \right\} \neq 0.$$

APPENDIX APPENDIX C. PROOF OF ERROR MODEL COMPOSITION LEMMAS

We first prove Lemma C.1 to pave the path to the proofs of other lemmas.

Lemma C.1. *There exist a solution a_1, a_2, b_1, b_2 for a system of equations,*

(21)
$$\begin{cases} a_1^2 + a_2^2 = s \\ b_1^2 + b_2^2 = t \\ a_1 b_1 + a_2 b_2 = r \end{cases}$$

where $0 \leq s, t \leq 1$, and $st \geq r^2$.

Proof. Due to the fact that $0 \leq s, t \leq 1$, we could parametrize a_1, a_2, b_1, b_2 as

$$a_1 = \sqrt{s} \cos \theta, \quad a_2 = \sqrt{s} \sin \theta,$$
$$b_1 = \sqrt{t} \cos \phi, \quad b_2 = \sqrt{t} \sin \phi.$$

The last equation in (21) then admits,

$$\sqrt{st} \cos(\theta - \phi) = r.$$

Since $st \geq r^2$, we have $-1 \leq \frac{r}{\sqrt{st}} \leq 1$. Hence, there is a unique solution for $\theta - \phi$. Therefore, the system of equations (21) has infinitely many solutions.

$\square$

Proof of Lemma 2.1. We denote

$$A_j = 1 - a_{j3}^2 - b_{j3}^2,$$
$$B_j = b_{j3}^2,$$
$$C_j = a_{j1} b_{j1} + a_{j2} b_{j2},$$

for $j = 1, 2$. The Kraus error model (3) then could be written as

$$K_j(\rho) = \begin{pmatrix} A_j r_{11} + B_j & C_j r_{12} \\ C_j r_{21} & 1 - A_j r_{11} - B_j \end{pmatrix},$$

where

$$\rho = \begin{pmatrix} r_{11} & r_{12} \\ r_{21} & r_{22} \end{pmatrix},$$

and $\operatorname{tr}(\rho) = 1$. The composition of K_1 and K_2 admits,

$$K_2(K_1(\rho)) = \begin{pmatrix} A_1 A_2 r_{11} + B_1 A_2 + B_2 & C_1 C_2 r_{12} \\ C_1 C_2 r_{21} & 1 - A_1 A_2 r_{11} - B_1 A_2 - B_2 \end{pmatrix}.$$

Therefore, by requiring the parameters $a_1, b_1, a_2, b_2, a_3, b_3$ satisfying

(22)
$$\begin{cases} A_1 A_2 = 1 - a_3^2 - b_3^2 = a_1^2 + a_2^2 + b_1^2 + b_2^2 - 1 \\ B_1 A_2 + B_2 = b_3^2 = 1 - b_1^2 - b_2^2 \\ C_1 C_2 = a_1 b_1 + a_2 b_2 \end{cases},$$

we are sure that the Kraus error is in the form of (4) and satisfies $K = K_2 \circ K_1$. We rearrange (22) and obtain,

$$\begin{cases} a_1^2 + a_2^2 = A_1 A_2 + B_1 A_2 + B_2 \\ b_1^2 + b_2^2 = 1 - B_1 A_2 - B_2 \\ a_1 b_1 + a_2 b_2 = C_1 C_2 \end{cases} .$$

We first notice that

$$A_1 A_2 + B_1 A_2 + B_2 = 1 - (1 - a_{13}^2)a_{23}^2 - (1 - b_{23}^2)a_{13}^2 \le 1,$$

and

$$A_1 A_2 + B_1 A_2 + B_2 \ge a_{13}^2 a_{23}^2 + a_{13}^2 b_{23}^2 \ge 0,$$

where the second inequality adopts the assumption $a_{13}^2 + a_{23}^2 \le 1$.

We also have,

$$1 - B_1 A_2 - B_2 = 1 - b_{13}^2(1 - a_{23}^2) - b_{23}^2(1 - b_{13}^2) \le 1,$$

and

$$1 - B_1 A_2 - B_2 \ge b_{13}^2 a_{23}^2 + b_{13}^2 b_{23}^2 \ge 0,$$

where the second inequality adopts the assumption $b_{13}^2 + b_{23}^2 \le 1$.

Using the Cauchy inequality, we obtain

$$(C_1 C_2)^2 \le \left(a_{11}^2 + a_{12}^2\right)\left(b_{11}^2 + b_{12}^2\right)\left(a_{21}^2 + a_{22}^2\right)\left(b_{21}^2 + b_{22}^2\right)$$
$$= \left(1 - a_{13}^2\right)\left(1 - b_{13}^2\right)\left(1 - a_{23}^2\right)\left(1 - b_{23}^2\right),$$

and, hence,

$$(A_1 A_2 + B_1 A_2 + B_2)\left(1 - B_1 A_2 - B_2\right) - (C_1 C_2)^2$$
$$\ge a_{13}^2 b_{23}^2 \left(1 - b_{13}^2 - b_{23}^2\right) + a_{23}^2 b_{13}^2 \left(1 - a_{13}^2 - a_{23}^2\right) + a_{13}^2 b_{13}^2 \left(a_{23}^4 + a_{23}^2 b_{23}^2 + b_{23}^4\right) \ge 0.$$

Finally, by Lemma C.1, we know that (22) has solutions and $K_2 \circ K_1$ can be in the form of (4).
$\qquad\square$

Proof of Lemma 2.2. We simply have

(23) $\qquad K_2 \circ K_1 = (K_{11} \otimes K_{21}) \circ (K_{12} \otimes K_{22}) = (K_{11} \circ K_{12}) \otimes (K_{21} \circ K_{22}),$

which is a double-qubit Kraus model in the form of (5). $\qquad\square$

Proof of Lemma 2.3. The X, Y, Z errors work on a density matrix

$$\rho = \begin{pmatrix} r_{11} & r_{12} \\ r_{21} & r_{22} \end{pmatrix}$$

as

$$X\rho X = \begin{pmatrix} r_{22} & r_{21} \\ r_{12} & r_{11} \end{pmatrix}, Y\rho Y = \begin{pmatrix} r_{22} & -r_{21} \\ -r_{12} & r_{11} \end{pmatrix}, Z\rho Z = \begin{pmatrix} r_{11} & -r_{12} \\ -r_{21} & r_{22} \end{pmatrix}.$$

Thus, the density matrix with errors is

$$\tilde{\rho} = p_I \rho + p_X X \rho X + p_Y Y \rho Y + p_Z Z \rho Z + p_{R0} \left|0\rangle\langle0\right| + p_{R1} \left|1\rangle\langle1\right| + \frac{p_D I}{2}$$

$$= \begin{pmatrix} (p_I + p_Z) r_{11} + (p_X + p_Y) r_{22} + p_{R0} + \frac{p_D}{2} & (p_X - p_Y) r_{21} + (p_I - p_Z) r_{12} \\ (p_X - p_Y) r_{12} + (p_I - p_Z) r_{21} & (p_I + p_Z) r_{22} + (p_X + p_Y) r_{11} + p_{R1} + \frac{p_D}{2} \end{pmatrix}$$

$$= \begin{pmatrix} (p_I + p_Z - p_X - p_Y) r_{11} + p_X + p_Y + p_{R0} + \frac{p_D}{2} & (p_I - p_Z) r_{12} \\ (p_I - p_Z) r_{21} & \frac{p_D}{2} - (p_I + p_Z - p_X - p_Y) r_{11} + p_I + p_Z + p_{R1} \end{pmatrix}.$$

The last equality makes use of $p_X = p_Y$ and $r_{11} + r_{22} = \mathrm{tr}\,(\rho) = 1$. On the other hand, the Kraus error (3) works as

$$K_{\mathrm{sq}}(\rho) = \begin{pmatrix} (a_1^2 + a_2^2 + b_1^2 + b_2^2 - 1) r_{11} + 1 - b_1^2 - b_2^2 & (a_1 b_1 + a_2 b_2) r_{12} \\ (a_1 b_1 + a_2 b_2) r_{21} & -(a_1^2 + a_2^2 + b_1^2 + b_2^2 - 1) r_{11} + b_1^2 + b_2^2 \end{pmatrix}.$$

Therefore, as long as it holds

$$(24) \qquad \begin{cases} a_1^2 + a_2^2 = p_I + p_Z + p_{R0} + \frac{p_D}{2} \\ b_1^2 + b_2^2 = p_I + p_Z + p_{R1} + \frac{p_D}{2} \\ a_1 b_1 + a_2 b_2 = p_I - p_Z \end{cases},$$

the probabilistic error is equivalent to the Kraus error. By construction, we have

$$0 \leq p_I + p_Z + p_{R0} + \frac{p_D}{2} \leq 1,$$

$$0 \leq p_I + p_Z + p_{R1} + \frac{p_D}{2} \leq 1.$$

In addition, we have,

$$\left(p_I + p_Z + p_{R0} + \frac{p_D}{2}\right)\left(p_I + p_Z + p_{R1} + \frac{p_D}{2}\right) \geq p_I^2 + p_Z^2 \geq (p_I - p_Z)^2.$$

Finally, by Lemma C.1, we know that (24) has solutions and probabilistic error can be in the form of (4).

$\square$

Appendix Appendix D. Linear growing error bound

Proof of Lemma 2.4. Suppose the corresponding unitary matrix of gate G_k is U_k, then error-free density matrices are shown in (7), while the actual states can also be written explicitly as

$$\tilde{\rho}_0 = \rho_0,$$

$$\tilde{\rho}_1 = K_1 \left(U_1 \tilde{\rho}_0 U_1^\dagger\right),$$

$$\cdots$$

$$\tilde{\rho}_m = K_m \left(U_m \tilde{\rho}_{m-1} U_m^\dagger\right).$$

By the assumption (8), we have

$$
\begin{aligned}
\|\tilde{\rho}_k - \rho_k\|_{\mathrm{F}} &= \left\| K_k \left(U_k \tilde{\rho}_{k-1} U_k^\dagger \right) - U_k \rho_{k-1} U_k^\dagger \right\|_{\mathrm{F}} \\
&= \left\| K_k \left(U_k \tilde{\rho}_{k-1} U_k^\dagger \right) - U_k \tilde{\rho}_{k-1} U_k^\dagger + U_k \tilde{\rho}_{k-1} U_k^\dagger - U_k \rho_{k-1} U_k^\dagger \right\|_{\mathrm{F}} \\
&\leq \left\| K_k \left(U_k \tilde{\rho}_{k-1} U_k^\dagger \right) - U_k \tilde{\rho}_{k-1} U_k^\dagger \right\|_{\mathrm{F}} + \left\| U_k \tilde{\rho}_{k-1} U_k^\dagger - U_k \rho_{k-1} U_k^\dagger \right\|_{\mathrm{F}} \\
&\leq \gamma_1 + \|\tilde{\rho}_{k-1} - \rho_{k-1}\|_{\mathrm{F}}.
\end{aligned}
$$

Recursively applying (25), we obtain,

$$
\|\tilde{\rho}_m - \rho_m\|_{\mathrm{F}} \leq \gamma_1 + \|\tilde{\rho}_{m-1} - \rho_{m-1}\|_{\mathrm{F}} \leq 2\gamma_1 + \|\tilde{\rho}_{m-2} - \rho_{m-2}\|_{\mathrm{F}} \leq \cdots \leq m\gamma_1.
$$

$\square$

Proof. For general probabilistic model (10), it holds

$$
\begin{aligned}
\|P(\rho) - \rho\|_{\mathrm{F}} &= \left\| p\rho + (1-p)R\rho R^\dagger - \rho \right\|_{\mathrm{F}} \\
&\leq (1-p)\left(\|\rho\|_{\mathrm{F}} + \left\| R\rho R^\dagger \right\|_{\mathrm{F}} \right) \\
&\leq 2(1-p).
\end{aligned}
$$

Choosing $\gamma_2 = 2 - 2\min\{p_1, \cdots, p_m\}$ and applying similar derivations as in the proof of Lemma 2.4, we have (11).

$\square$

Appendix Appendix E. Supporting Inequalities

We prove a few inequalities in this section, which are widely used throughout this paper.

Given two density matrices, $\tilde{\rho}$ and ρ, we have,

$$
\|\tilde{\rho} - \rho\|_{\mathrm{F}}^2 = \|\tilde{\rho}\|_{\mathrm{F}}^2 + \|\rho\|_{\mathrm{F}}^2 - 2\mathrm{tr}\left(\tilde{\rho}\rho\right) \leq 1 + 1 - 2\mathrm{tr}\left(\tilde{\rho}\rho\right) \leq 2,
$$

where the first inequality is due to the property of density matrix, and the second inequality is due to Ruhe's trace inequality.

Given two density matrices, $\tilde{\rho}$ and ρ, and a Kraus operator K, we have,

$$
(26) \qquad \|K(\tilde{\rho}) - \rho\|_{\mathrm{F}}^2 = \|K(\tilde{\rho})\|_{\mathrm{F}}^2 + \|\rho\|_{\mathrm{F}}^2 - 2\mathrm{tr}\left(K(\tilde{\rho})\rho\right) \leq 1 + 1 - 2\mathrm{tr}\left(K(\tilde{\rho})\rho\right) \leq 2,
$$

where the first inequality is partially due to the property of density matrix, and the second inequality is due to Ruhe's trace inequality. Since the Kraus operator preserves the trace and the semi-positivity of the matrix, we could show that $\|K(\tilde{\rho})\|_{\mathrm{F}}^2 \leq 1$, which is used in the first inequality in (26).

Appendix Appendix F. Kraus error model lemmas

For both Lemma 3.1 and Lemma 3.2, we would focus on the proof for density matrices of pure state and then adopt the inequality (27) to achieve the final inequalities. Given a density matrix ρ, we could always rewrite it as an eigenvalue decomposition,

$$
\rho = \sum_{i=1}^{N} \lambda_i u_i u_i^\dagger,
$$

where u_is are orthonormal vectors and λ_is are all non-negative. Further, we know that the density matrix is of trace one, i.e., $\operatorname{tr}(\rho) = 1$, which is equivalent to $\sum_i \lambda_i = 1$. By the linearity of Kraus operator and the triangle inequality of Frobenius norm, we have,

$$(27) \qquad \|K(\rho)\|_{\mathrm{F}} = \left\| \sum_{i=1}^{N} \lambda_i K(u_i u_i^\dagger) \right\|_{\mathrm{F}} \leq \sum_{i=1}^{N} \lambda_i \left\| K(u_i u_i^\dagger) \right\|_{\mathrm{F}} \leq \max_i \left\| K(u_i u_i^\dagger) \right\|_{\mathrm{F}}.$$

Hence, it is sufficient to show that Lemma 3.1 and Lemma 3.2 holds for the density matrices of pure state.

Firstly, we prove a lemma for n-qubit pure state density matrixs.

Lemma F.1. *We consider an n-qubit density matrix of a pure state*

$$(28) \qquad \rho = \begin{pmatrix} r_{11} & r_{12} & \cdots & r_{1N} \\ r_{21} & r_{22} & \cdots & r_{2N} \\ \vdots & \vdots & \ddots & \vdots \\ r_{N1} & r_{N2} & \cdots & r_{NN} \end{pmatrix} = \begin{pmatrix} R_{11} & R_{12} \\ R_{21} & R_{22} \end{pmatrix} = \begin{pmatrix} R_1 R_1^\dagger & R_1 R_2^\dagger \\ R_2 R_1^\dagger & R_2 R_2^\dagger \end{pmatrix},$$

where $R_{11}, R_{12}, R_{21}, R_{22} \in \mathbb{C}^{\frac{N}{2} \times \frac{N}{2}}$, and $R_1, R_2 \in \mathbb{C}^{\frac{N}{2}}$ form the state of the pure state. The matrix

$$(29) \qquad \rho' = \begin{pmatrix} \|R_{11}\|_{\mathrm{F}} & \|R_{12}\|_{\mathrm{F}} \\ \|R_{21}\|_{\mathrm{F}} & \|R_{22}\|_{\mathrm{F}} \end{pmatrix}$$

is a single-qubit density matrix of a pure state.

Proof. Both $R_{11} = R_1 R_1^\dagger$ and $R_{22} = R_2 R_2^\dagger$ are symmetric positive semi-definite matrices and of rank no greater than 1. Therefore, it holds

$$\operatorname{tr}(\rho') = \|R_{11}\|_{\mathrm{F}} + \|R_{22}\|_{\mathrm{F}} = \operatorname{tr}(R_{11}) + \operatorname{tr}(R_{22}) = \operatorname{tr}(\rho) = 1.$$

We also have

$$\|\rho'\|_{\mathrm{F}}^2 = \|R_{11}\|_{\mathrm{F}}^2 + \|R_{12}\|_{\mathrm{F}}^2 + \|R_{21}\|_{\mathrm{F}}^2 + \|R_{22}\|_{\mathrm{F}}^2 = \|\rho\|_{\mathrm{F}}^2 = 1.$$

By the construction of R_{12} and R_{21}, we know that ρ' is a symmetric matrix. Let the two real eigenvalues of ρ' be λ_1 and λ_2 ($\lambda_1 \geq \lambda_2$). The above equations are equivalent to,

$$\lambda_1 + \lambda_2 = 1, \quad \lambda_1^2 + \lambda_2^2 = 1,$$

whose solution is $\lambda_1 = 1$ and $\lambda_2 = 0$. Hence, ρ' is a single-qubit density matrix of a pure state.
$\square$

Now we prove Lemma 3.1.

Proof of Lemma 3.1. We first prove that Lemma 3.1 holds for single-qubit density matrix. Denote $\rho = uu^\dagger$, where $u = [u_1, u_2]^\top \in \mathbb{C}^2$ and $\|u\|^2 = 1$. Substituting the expression of $K_{\mathrm{sq}}(uu^\dagger)$ as in (3),

$$K_{\mathrm{sq}}(uu^\dagger) = V_1 uu^\dagger V_1^\dagger + V_2 uu^\dagger V_2^\dagger + V_3 uu^\dagger V_3^\dagger + V_4 uu^\dagger V_4^\dagger$$
$$= x_1 x_1^\dagger + x_2 x_2^\dagger + x_3 x_3^\dagger + x_4 x_4^\dagger,$$

where $x_k = V_k u$ for $k = 1, 2, 3, 4$, i.e.

$$x_1 = \begin{pmatrix} a_1 u_1 \\ b_1 u_2 \end{pmatrix}, \quad x_2 = \begin{pmatrix} a_2 u_1 \\ b_2 u_2 \end{pmatrix}, \quad x_3 = \begin{pmatrix} 0 \\ a_3 u_1 \end{pmatrix}, \quad x_4 = \begin{pmatrix} b_3 u_2 \\ 0 \end{pmatrix},$$

satisfying

$$\|x_1\|^2 + \|x_2\|^2 + \|x_3\|^2 + \|x_4\|^2 = u^\dagger \left(V_1^\dagger V_1 + V_2^\dagger V_2 + V_3^\dagger V_3 + V_4^\dagger V_4 \right) u = 1.$$

By the triangle inequality, we have

$$(30) \qquad \left\| K_{\mathrm{sq}} \left(uu^\dagger \right) \right\|_{\mathrm{F}} \leq \left\| x_1 x_1^\dagger \right\|_{\mathrm{F}} + \left\| x_2 x_2^\dagger \right\|_{\mathrm{F}} + \left\| x_3 x_3^\dagger \right\|_{\mathrm{F}} + \left\| x_4 x_4^\dagger \right\|_{\mathrm{F}} = 1.$$

Next, we would like to show that the equality in the inequality (30) cannot be achieved, i.e. $\left\| K_{\mathrm{sq}} \left(uu^\dagger \right) \right\|_{\mathrm{F}}$ is strictly less than 1 for any u. Let us consider the above triangle inequality for a pair x_i and x_j. The triangle inequality could be simplified as the Cauchy-Schwarz inequality,

$$(31) \qquad \left\| x_i x_i^\dagger + x_j x_j^\dagger \right\|_{\mathrm{F}} \leq \left\| x_i x_i^\dagger \right\|_{\mathrm{F}} + \left\| x_j x_j^\dagger \right\|_{\mathrm{F}} \Leftrightarrow \left| x_i^\dagger x_j \right| \leq |x_i|^2 |x_j|^2$$

where the equality is achieved if and only if x_i and x_j are linearly dependent. Further, the equality in (30) holds if and only if the equality in (31) holds for any pair x_i and x_j.

Recall that $\det \left\{ \begin{pmatrix} a_1 & a_2 \\ b_1 & b_2 \end{pmatrix} \right\} \neq 0$ as in (3). When $u_1 = 0$, by the normality of u, we know that $|u_2| = 1$. x_1, x_2 and x_4 cannot be linearly dependent unless $b_1 = b_2 = b_3 = 0$, which violates the assumption. When $u_2 = 0$, similar analysis leads to $a_1 = a_2 = a_3 = 0$, which also violates the assumption. When $u_1 \neq 0$ and $u_2 \neq 0$, by the linear dependency of x_3 and x_4, we know that $a_3 = b_3 = 0$. In this case, the linear dependency of x_1 and x_2 contradicts the nonzero determinant assumption. Therefore, $\left\| K_{\mathrm{sq}} \left(uu^\dagger \right) \right\|_{\mathrm{F}}$ is strictly less than 1.

Since $\left\| K_{\mathrm{sq}} \left(uu^\dagger \right) \right\|_{\mathrm{F}}$ is a continuous function of u_1 and u_2, which are defined on a compact domain $|u_1|^2 + |u_2|^2 = 1$, the supremum of $\left\| K_{\mathrm{sq}} \left(uu^\dagger \right) \right\|_{\mathrm{F}}$ is achievable and is strictly less than 1. Thus, there is a $\delta' > 0$, such that $\left\| K_{\mathrm{sq}} \left(uu^\dagger \right) \right\|_{\mathrm{F}}^2 \leq 1 - \delta'$ for pure state single-qubit density matrix $\rho = uu^\dagger$. Via the inequality (27), we know that there exists a $\delta > 0$, such that $K_{\mathrm{sq}} (\rho) \leq 1 - \delta$ for all single-qubit density matrix ρ.

Now we consider an n-qubit pure state density matrix in the form of (28). Without loss of generality, we assume that the Kraus operator is acted on the first qubit, then

$$K_{\mathrm{sq}} (\rho) = \sum_{j=1}^{4} (V_j \otimes I) \rho \left(V_j^\dagger \otimes I \right)$$

$$= \begin{pmatrix} b_3^2 R_{22} + \left(a_1^2 + a_2^2 \right) R_{11} & (a_1 b_1 + a_2 b_2) R_{12} \\ (a_1 b_1 + a_2 b_2) R_{21} & a_3^2 R_{11} + \left(b_1^2 + b_2^2 \right) R_{22} \end{pmatrix}.$$

Using triangle inequality, we have

$$
\begin{aligned}
\left\| K_{\mathrm{sq}}\left(\rho\right) \right\|_{\mathrm{F}}^{2} &= \left\| b_3^2 R_{22} + \left(a_1^2 + a_2^2\right) R_{11} \right\|_{\mathrm{F}}^{2} + \left\| \left(a_1 b_1 + a_2 b_2\right) R_{12} \right\|_{\mathrm{F}}^{2} \\
&\quad + \left\| a_3^2 R_{11} + \left(b_1^2 + b_2^2\right) R_{22} \right\|_{\mathrm{F}}^{2} + \left\| \left(a_1 b_1 + a_2 b_2\right) R_{21} \right\|_{\mathrm{F}}^{2} \\
&\leq \left(b_3^2 \left\| R_{22} \right\|_{\mathrm{F}} + \left(a_1^2 + a_2^2\right) \left\| R_{11} \right\|_{\mathrm{F}} \right)^{2} + \left(a_1 b_1 + a_2 b_2\right)^2 \left\| R_{12} \right\|_{\mathrm{F}}^{2} \\
&\quad + \left(a_3^2 \left\| R_{11} \right\|_{\mathrm{F}} + \left(b_1^2 + b_2^2\right) \left\| R_{22} \right\|_{\mathrm{F}} \right)^{2} + \left(a_1 b_1 + a_2 b_2\right)^2 \left\| R_{21} \right\|_{\mathrm{F}}^{2} \\
&= \left\| K_{\mathrm{sq}}\left(\rho'\right) \right\|_{\mathrm{F}}^{2},
\end{aligned}
$$

where

$$
\rho' = \begin{pmatrix} \left\| R_{11} \right\|_{\mathrm{F}} & \left\| R_{12} \right\|_{\mathrm{F}} \\ \left\| R_{21} \right\|_{\mathrm{F}} & \left\| R_{22} \right\|_{\mathrm{F}} \end{pmatrix},
$$

and we abuse notation $K_{\mathrm{sq}}\left(\rho'\right)$ denoting K_{sq} acting on ρ'. According to Lemma F.1, ρ' is a single-qubit pure state density matrix. Therefore, it holds $\left\| K_{\mathrm{sq}}\left(\rho\right) \right\|_{\mathrm{F}}^{2} \leq \left\| K_{\mathrm{sq}}\left(\rho'\right) \right\|_{\mathrm{F}}^{2} \leq 1 - \delta'$ for some constant δ'. Again, via the inequality (27), we know that there exists a $\delta > 0$, such that $K_{\mathrm{sq}}\left(\rho\right) \leq 1 - \delta$ for all density matrix ρ.

$\square$

Lemma 3.2 can be proved in the same way as that of Lemma 2.1. For the sake of space, we omit the detailed proof.

(ZY) School of Mathematical Sciences, Shanghai Jiao Tong University, Shanghai, China.
Email address: `yuziang@sjtu.edu.cn`

(YL) School of Mathematical Sciences, Fudan University, Shanghai, China.
Email address: `yingzhouli@fudan.edu.cn`